Title

A case of well differentiated cholangiolocellular carcinoma visualized with contrast-enhanced ultrasonography using Sonazoid™

Satoru Joshita [1)], Tetsuya Ichijo [1)], Fumitaka Suzuki [2)], Takahide Yokoyama [2)], Yukiko Sugiyama [3)], Mana Fukushima [4)], Atsushi Kamijo [1)], Michiharu Komatsu [1)], Takeji Umemura [1)], Kaname Yoshizawa [1)], Shinichi Miyagawa [2)], Eiji Tanaka [1)]

1) Department of Internal Medicine, Division of Gastroenterology and Hepatology, Shinshu University School of Medicine, Matsumoto, Japan

2) Department of Surgery, Shinshu University School of Medicine, Matsumoto, Japan

3) Department of Radiology, Shinshu University School of Medicine, Matsumoto, Japan

4) Department of Laboratory Medicine, Shinshu University Hospital, Matsumoto, Japan

Running title: Imaging features of cholangiolocellular carcinoma

Corresponding author: Satoru Joshita M.D., Department of Internal Medicine, Division of Gastroenterology and Hepatology, Shinshu University School of Medicine, 3-1-1 Asahi, Matsumoto, 390-8621, Japan.

E-mail: joshita@shinshu-u.ac.jp

Tel.: +81-263-37-2634

Fax: +81-263-32-9412

Abstract

Here we report the first case of cholangiolocellular carcinoma (CoCC) visualized with contrast-enhanced ultrasonography (CEUS) using a second-generation contrast agent, Sonazoid™. A 76-year-old man was admitted to our hospital for evaluation of a hepatic tumor. The tumor was described to have hyper-enhancement in the early phase and persistent enhancement in the late phase by contrast-enhanced computed tomography (CT) and magnetic resonance imaging (MRI), as well as hypervascularity by angiography. CEUS assessment of the nodule showed diffuse and homogeneous enhancement in the pure arterial phase, which became progressively hypoechoic relative to the adjacent liver parenchyma during the portal vein and late phases (mixed vascular phase), and showed a contrast defect with unclear border in the Kupffer phase. We histologically diagnosed this hepatic tumor as CoCC. In light of the above findings and the rarity of CoCC, it is helpful to incorporate the results of several imagings, such as CT, MRI, angiography, and CEUS with a second-generation contrast agent, when clinically diagnosing CoCC.

Key words: cholangiolocellular carcinoma; contrast-enhanced ultrasonography;

second-generation contrast agent; Sonazoid™

Introduction

Cholangiolocellular carcinoma (CoCC) was first reported as an adenocarcinoma originating from the ductules/canals of Hering. [1] Considered to be derived from hepatic stem cell carcinoma [2], CoCC is categorized as a subtype of cholangiocellular carcinoma (CCC) based on criteria from the World Health Organization. [3] In Japan, CoCC was recently classified as an independent primary liver cancer in 2008. [4] CoCC has been reported to account for approximately 1% of primary liver cancers. [1] In a Japanese study, four cases of CoCC were found in 708 (0.56%) consecutively resected cases of primary liver cancer. [5] CoCC can be clinically misdiagnosed as hepatocellular carcinoma (HCC) because many patients are infected with hepatitis C or B virus. [6] Furthermore, the features of CoCC in ultrasonography have not been fully elucidated.

Contrast-enhanced ultrasonography (CEUS) is a useful tool for the diagnosis of hepatic tumors [7], evaluation of malignancy grade and treatment response, and CEUS-guided percutaneous local ablation therapy. [7-9] Injection of Sonazoid™ (perfluorobutane)[10], a second-generation contrast agent for ultrasonography, was approved in Japan for imaging lesions associated with hepatic cancer via ultrasound in 2007. However, due to the rarity of CoCC, few studies combining the

findings of CEUS, MRI, CT, and angiography have been reported. As such, we here present a case of CoCC that showed interesting findings under CEUS using Sonazoid™.

Case

A 76-year-old man was admitted to our hospital for examination of a hepatic tumor located from segment 4 to 8. He had regularly seen a doctor since the onset of chronic hepatitis C at 60 years of age. The nodular lesion was 10 mm in diameter and was first detected with B-mode ultrasonography (US) and computed tomography (CT) three years before admission, but had since changed in neither size nor imaging characteristics. The size of the tumor began slowly enlarging 5 months before admission.

Physical examination on admission was normal. Laboratory tests were also normal and were as follows: white blood cell count, 5,340 /mm^3; red blood cell count, 483x10^4 /mm^3; platelet count, 145,000 /mm^3; prothrombin time (percent), 94.7%; albumin, 4.6 g/dl; total bilirubin, 1.1 mg/dl; aspartate aminotransferase, 19 U/l; alanine aminotransferase, 21 U/l; alkaline phosphatase, 189 U/l; and gamma-glutamyl transpeptidase, 24 U/l. Hepatitis B virus surface antigen was

negative and core antibody was low strength positive. The levels of several serum tumor markers were all within normal limits, including alpha-fetoprotein, 1.3 ng/ml; prothrombin induced by vitamin K absence or antagonist II, 13 mAU/ml; carcinoembryonic antigen, 2.1 ng/ml; and carbohydrate antigen 19-9, 20.7 U/ml.

The hepatic nodule appeared as a heterogeneous hypoechoic lesion with unclear border in which the middle hepatic vein was seen running through it in B-mode US (Figure 1a) and Doppler US (EUB-8500, Hitachi Medical Co., Ltd., Japan). An abdominal CT (LightSpeed VCT, GE Healthcare, United States) showed a 28 mm-wide tumor with lobulated edge, diffuse homogeneous enhancement in the early phase, and persistent enhancement in the delayed phase of dynamic contrast imaging (Figure 2a-2c). Magnetic resonance imaging (MRI) (Trio Tim, Siemens Medical Solution, Germany) showed low and high intensity nodules in T1 and T2 weighted imaging with fat suppression, respectively (Figure 2d, 2e), with a capsule-like lesion having a mosaic pattern in early contrast enhancement and persistent enhancement in the delayed phase (Figure 2f-2i). The tumor showed no decrease in signal intensity in T2 weighted images by superparamagnetic iron oxide magnetic resonance imaging

(SPIO-MRI) (Figure 2j), and was seen as feeding from the hepatic artery (A8) in both angiography and CT during hepatic arteriography (CTA). It also had enhanced persistency in the equilibrium phase of angiography, and revealed a complete contrast defect in CT during arterial portography (CTAP) (Figure 3). These findings suggested that the tumor was neither common HCC nor CCC. We next performed CEUS using harmonic US and a bolus injection of 0.015 mL/kg Sonazoid™ and found a more extensive tumor area than the one shown in B-mode US that was diffusely and homogeneously enhanced from 10 to 40 seconds in the pure arterial phase. The lesion became progressively hypoechoic relative to the adjacent liver parenchyma during the portal vein and late phases (mixed vascular phase), and provided a contrast defect with unclear border in the postvascular Kupffer phase (Figure 1b-1e).

The tumor invasively proliferated in a duct-like configuration without production of mucinous fluid in a tissue specimen taken by US-guided biopsy. As the tumor had mild atypia, immunostaining of hepatocyte paraffin 1 (Hep par 1), cytokeratin (CK) 7, CK 19, epithelial membrane antigens (EMA), and neural cell adhesion molecule (NCAM) were negative, positive, slightly positive, strongly positive intraluminally but negative in the cytoplasm, and slightly positive, respectively. We

thus histologically diagnosed the tumor as being well-differentiated CoCC. (Figure 4a-4d)

The patient had a relative contraindication for surgical tumor resection because of high risks of cerebrovascular complications due to cervical arteriosclerosis and his past history of asymptomatic lacunar infarction detected by brain MRI in preoperative analysis. The patient first opted for transcatheter arterial embolization (TAE) despite warnings that TAE might have no effect on this type of tumor. Indeed, no changes were seen one month later. After informing him about the risk of cerebrovascular complications of surgery, we obtained informed consent and performed expanded anterior segmentectomy of the liver with lymph node dissection. The histological diagnosis after surgery was the same as the tumor biopsy.

Discussion

The clinical and imaging features of CoCC have not been fully characterized because only a small number of cases have been previously reported. [5, 6, 11-13] Most CoCC cases have hyper-enhancement in the early phase of contrast enhanced CT or MRI and hypervascularity in angiography. [6, 13] Persistent

enhancement in the late phase of contrast enhanced CT or MRI was also depicted in some cases, [5, 6, 11-13] reflecting slow diffusion of the contrast agent into the fibrotic component of the tumor similarly seen in cases with CCC. [14]

This study is the first to present findings of CoCC using ultrasonography with injection of Sonazoid™. Sonazoid™ is a second-generation ultrasound contrast agent consisting of perfluorobutane gas microspheres stabilized by a membrane of hydrogenated egg phosphatidyl serine, which imparts more persistency in the blood stream after injection than first-generation contrast agents. [15] In particular, Sonazoid™ enables stabilized images for more than 10 minutes after injection in the Kupffer phase, stemming from phagocytosis or trapping of the Sonazoid™ microspheres by Kupffer cells. [15, 16] Thus, common HCC and other metastatic hepatic tumors present as contrast defect images in the Kupffer phase because they contain no Kupffer cells, unlike the surrounding hepatic parenchyma. [17, 18] This was also the case in our patient; a contrast defect was seen in the Kupffer phase during CEUS.

In a report of overt HCC visualized using Sonazoid™, a pure arterial supply was seen in the pure arterial phase, hypervascularity in the mixed vascular phase, and a contrast defect in the Kupffer phase. [17] Similar characteristics in the arterial

phase of this case were observed in that we recognized the tumor with strongly homogeneous hyperperfusion which was induced by blood pooling; assessment of microvessel density using immonohistochemical staining of the biopsy specimen for specific endothelial cell markers, such as CD 34, [19] showed an abundance of capillary endothelial vessels in the tumor. (Figure 4e) On the other hand, one report on common HCC using Sonazoid™ showed fast washout in the late vascular phase three minutes after injection of Sonazoid™. [18] Visualization of CCC using Sonazoid™ has not yet been reported in English literature. However, it has been reported using other second-generation contrast agents, and perfusion images of almost all cases revealed hyperperfusion in the arterial phase [20, 21], followed by punched-out contrast defects and relatively rapid washout in subsequent portal and/or sinusoidal phases. [20] The characteristics of this case in the mixed vascular phase are comparable to those of common HCC and CCC in that washout relatively earlier in the mixed vascular phase was described. We cannot generalize that all cases of CoCC show hyperperfusion in the arterial phase, relatively rapid washout in the mixed phase, and complete contrast defect in the Kupffer phase because CoCC can show several pathologically different patterns. [22] Furthermore, more cases and comparisons with hepatocellular

carcinoma and cholangiocellular carcinoma are needed to better characterize the images of CEUS with Sonazoid™. Nonetheless, consideration of these CEUS findings should be helpful to elevate diagnostic accuracy in patients with CoCC.

In conclusion, our case of CoCC showed homogeneous hyperperfusion in the arterial phase, relatively rapid washout in the mixed vascular phase, and then contrast defect with unclear border in the Kupffer phase using Sonazoid™ as a contrast agent. Clinicians should consider a hepatic tumor to be CoCC when the tumor simultaneously presents phenomena of both HCC and CCC in imaging tests. Incorporating findings from CEUS with those of CT, MRI, and angiography will be helpful to better diagnose CoCC. Further studies are needed to clarify the clinical and clinicopathological features of CoCC.

Acknowledgement

We thank Trevor Ralph for his editorial assistance.

References

1 Steiner PE, Higginson J. Cholangiolocellular carcinoma of the liver. Cancer. 1959 Jul-Aug;12: 753-9.

2 Theise ND, Saxena R, Portmann BC, et al. The canals of Hering and hepatic stem cells in humans. Hepatology. 1999 Dec;30: 1425-33.

3 Hirohashi S, Ishak K, Kojiro M, Wanless I, Theise N, Tsukuma H. Tumours of the liver and intrahepatic bile ducts. In: Hamilton SR, Aaltonen LA, eds. *Pathology and Genetics of Tumours of the Digestive System*. Lyon: International Agency for Research on Cancer (IARC) Press 2000; 257-02.

4 Japan LCSGo. The General Rules for the Clinical and Pathological Study of Primary Liver Cancer. Tokyo: Kanehara & Co., LTD. 2008.

5 Shiota K, Taguchi J, Nakashima O, Nakashima M, Kojiro M. Clinicopathologic study on cholangiolocellular carcinoma. Oncol Rep. 2001 Mar-Apr;8: 263-8.

6 Kanamoto M, Yoshizumi T, Ikegami T, et al. Cholangiolocellular carcinoma containing hepatocellular carcinoma and cholangiocellular carcinoma, extremely rare tumor of the liver:a case report. J Med Invest. 2008 Feb;55: 161-5.

7 Quaia E, Calliada F, Bertolotto M, et al. Characterization of focal liver lesions with contrast-specific US modes and a sulfur hexafluoride-filled microbubble contrast agent: diagnostic performance and confidence. Radiology. 2004 Aug;232: 420-30.

8 Minami Y, Kudo M, Chung H, et al. Contrast harmonic sonography-guided radiofrequency ablation therapy versus B-mode sonography in hepatocellular carcinoma: prospective randomized controlled trial. AJR Am J Roentgenol. 2007 Feb;188: 489-94.

9 Numata K, Morimoto M, Ogura T, et al. Ablation therapy guided by contrast-enhanced sonography with Sonazoid for hepatocellular carcinoma lesions not detected by conventional sonography. J Ultrasound Med. 2008 Mar;27: 395-406.

10 Forsberg F, Piccoli CW, Liu JB, et al. Hepatic tumor detection: MR imaging and conventional US versus pulse-inversion harmonic US of NC100100 during its reticuloendothelial system-specific phase. Radiology. 2002 Mar;222: 824-9.

11 Yamamoto M, Takasaki K, Nakano M, Saito A. Hepatic recurrence of cholangiolocellular carcinoma: report of a case. Hepatogastroenterology. 1996

Jul-Aug;43: 1046-50.
12 Fukukura Y, Hamanoue M, Fujiyoshi F, et al. Cholangiolocellular carcinoma of the liver: CT and MR findings. J Comput Assist Tomogr. 2000 Sep-Oct;24: 809-12.
13 Matsuda M, Hara M, Suzuki T, Kono H, Fujii H. Synchronously resected double primary hepatic cancers - hepatocellular carcinoma and cholangiolocellular carcinoma. J Hepatobiliary Pancreat Surg. 2006;13: 571-6.
14 Lacomis JM, Baron RL, Oliver JH, 3rd, Nalesnik MA, Federle MP. Cholangiocarcinoma: delayed CT contrast enhancement patterns. Radiology. 1997 Apr;203: 98-104.
15 Sontum PC. Physicochemical characteristics of Sonazoid, a new contrast agent for ultrasound imaging. Ultrasound Med Biol. 2008 May;34: 824-33.
16 Yanagisawa K, Moriyasu F, Miyahara T, Yuki M, Iijima H. Phagocytosis of ultrasound contrast agent microbubbles by Kupffer cells. Ultrasound Med Biol. 2007 Feb;33: 318-25.
17 Kudo M. New sonographic techniques for the diagnosis and treatment of hepatocellular carcinoma. Hepatol Res. 2007 Sep;37 Suppl 2: S193-9.
18 Hatanaka K, Kudo M, Minami Y, et al. Differential diagnosis of hepatic tumors: value of contrast-enhanced harmonic sonography using the newly developed contrast agent, Sonazoid. Intervirology. 2008;51 Suppl 1: 61-9.
19 Sasano H, Suzuki T. Pathological evaluation of angiogenesis in human tumor. Biomed Pharmacother. 2005 Oct;59 Suppl 2: S334-6.
20 Celli N, Gaiani S, Piscaglia F, et al. Characterization of liver lesions by real-time contrast-enhanced ultrasonography. Eur J Gastroenterol Hepatol. 2007 Jan;19: 3-14.
21 Dietrich CF. Characterisation of focal liver lesions with contrast enhanced ultrasonography. Eur J Radiol. 2004 Jun;51 Suppl: S9-17.
22 Komuta M, Spee B, Vander Borght S, et al. Clinicopathological study on cholangiolocellular carcinoma suggesting hepatic progenitor cell origin. Hepatology. 2008 May;47: 1544-56.

Figure Legends

Fig. 1. a) B-mode ultrasonography showed the hepatic nodule as a heterogeneous hypoechoic lesion with unclear border in which the middle hepatic vein was seen running through it. b-e) Contrast enhanced ultrasonography. (b: 26 seconds (pure arterial phase) after contrast agent injection, the nodule showed homogeneous hyper-enhancement without invasion of vessels in and around the tumor. c: 90 seconds (portal vein phase) after contrast agent administration, the tumor was isoechoic with the surrounding tissue. d: During the late phase (180 seconds after injection) the nodule became hypoechoic relative to the liver parenchyma. e: In Kupffer phase imaging (10 minutes after injection), it showed a contrast defect with unclear border.)

Fig. 2. a) Precontrast computed tomography (CT) depicted a hypoattenuating tumor (arrows) measuring 28 mm in diameter between the medial segment (S4) and anterior superior segment (S8) of the liver. b) It showed enhancement in the early phase of dynamic enhanced CT. c) It also showed persistent enhancement in the delayed phase. d-e) Magnetic resonance imaging (MRI) showed low and high intensity nodules in T1 and T2 weighted imaging with fat suppression, respectively. (d: T1 weighted images, e: T2 weighted images) f-i) MRI revealed

that the tumor (arrow heads) had mosaic pattern contrast enhancement in the early phase and persistent enhancement in the delayed phase. (f: 30 seconds, g: 60 seconds, h: 90 seconds, i: 120 seconds after injection of contrast agent) j) Superparamagnetic iron oxide magnetic resonance imaging showed that the rumor had no decrease in signal intensity in T2 weighted images.

Fig. 3. a) Angiographic examination showed a hypervascular tumor (arrows) fed by the anterior superior branch of the right hepatic artery (A8). b) The tumor had persistent enhancement in the equilibrium phase. c) CT during hepatic arteriography (CTA) showed that the tumor (arrow heads) was enhanced. d) Persistent enhancement was seen in the delayed phase. e) It was depicted as a complete contrast defect by CT during arterial portography (CTAP).

Fig. 4. a) Microscopic examination revealed that the tumor was a well differentiated adenocarcinoma. The tumor was composed of small ovoid nuclei and eosinophilic cytoplasm with mild atypia and proliferated in an anastomosing pattern of Hering's canal-like small glands with fibrous stroma. We could not see production of mucinous fluid in ducts. H & E, x100 b) Cells were immunohistologically negative to antibodies against hepatocyte paraffin 1 (Hep Par 1). x100 c) They also showed a strong intraluminal staining pattern of the

gland for epithelial membrane antigens (EMA). x100 d) Cells were slightly positive for cytokeratin 19. e) A number of capillary endothelial vessels stained with antibody for CD 34 antigens were seen in the cancerous part (arrows) compared with the non-cancerous part (arrowheads). x25

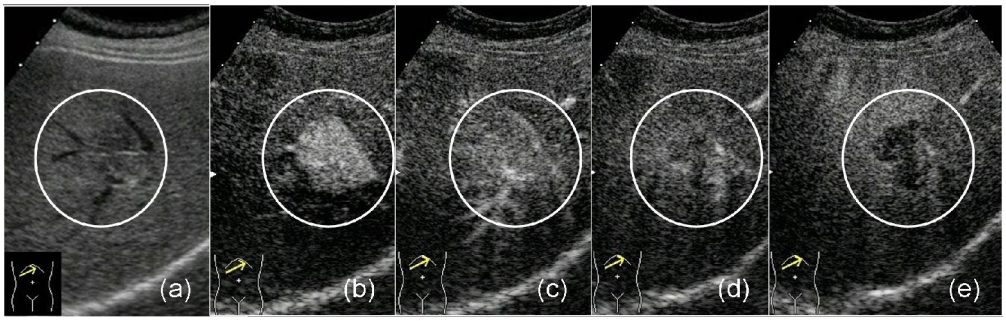

Fig. 1. a) B-mode ultrasonography showed the hepatic nodule as a heterogeneous hypoechoic lesion with unclear border in which the middle hepatic vein was seen running through it. b-e) Contrast enhanced ultrasonography. (b: 26 seconds (pure arterial phase) after contrast agent injection, the nodule showed homogeneous hyper-enhancement without invasion of vessels in and around the tumor. c: 90 seconds (portal vein phase) after contrast agent administration, the tumor was isoechoic with the surrounding tissue. d: During the late phase (180 seconds after injection) the nodule became hypoechoic relative to the liver parenchyma. e: In Kupffer phase imaging (10 minutes after injection), it showed a contrast defect with unclear border.)

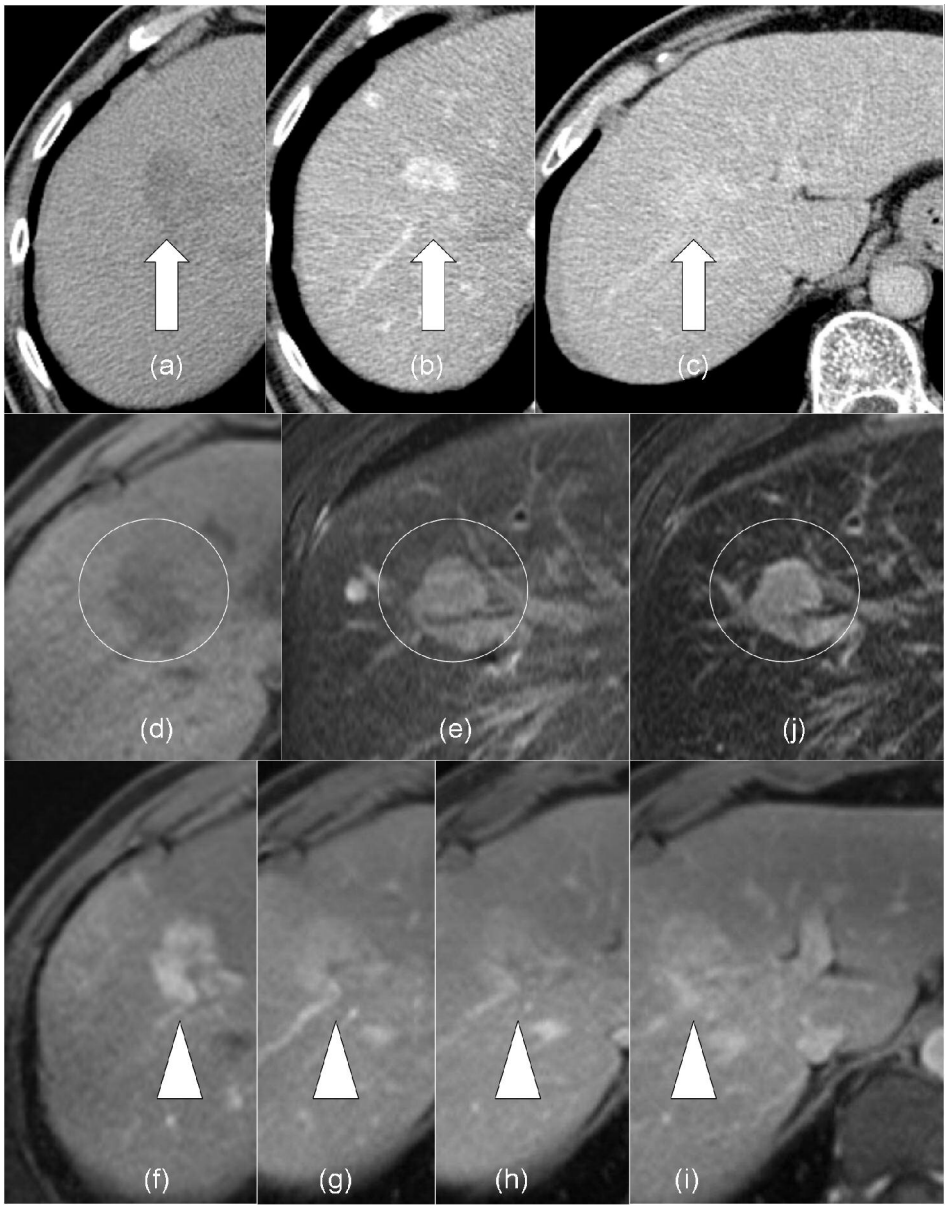

Fig. 2. a) Precontrast computed tomography (CT) depicted a hypoattenuating tumor (arrows) measuring 28 mm in diameter between the medial segment (S4) and anterior superior segment (S8) of the liver. b) It showed enhancement in the early phase of dynamic enhanced CT. c) It also showed persistent enhancement in the delayed phase. d-e) Magnetic resonance imaging (MRI) showed low and high intensity nodules in T1 and T2 weighted imaging with fat suppression, respectively. (d: T1 weighted images, e: T2 weighted images) f-i) MRI revealed that the tumor (arrow heads) had mosaic pattern contrast enhancement in the early phase and persistent enhancement in the delayed phase. (f: 30 seconds, g: 60 seconds, h: 90 seconds, i: 120 seconds after injection of contrast agent) j) Superparamagnetic iron oxide magnetic resonance imaging showed that the rumor had no decrease in signal intensity in T2 weighted images.

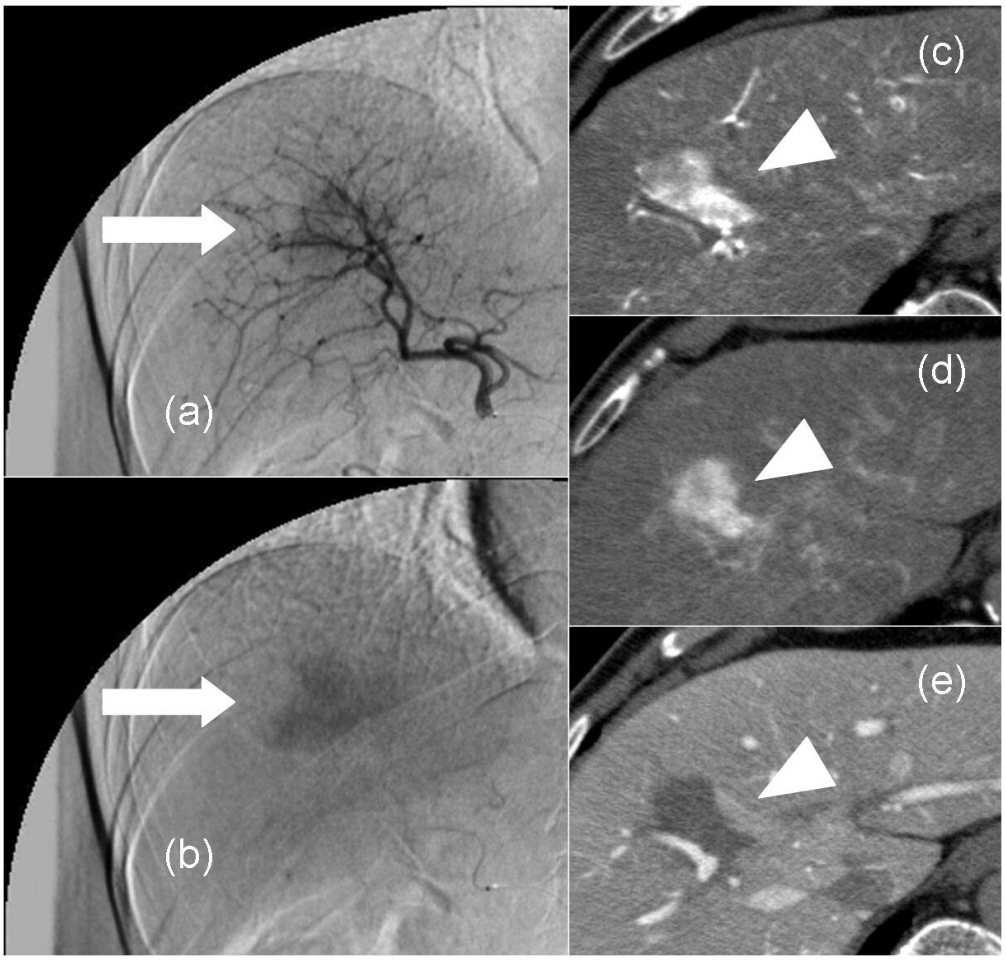

Fig. 3. a) Angiographic examination showed a hypervascular tumor (arrows) fed by the anterior superior branch of the right hepatic artery (A8). b) The tumor had persistent enhancement in the equilibrium phase. c) CT during hepatic arteriography (CTA) showed that the tumor (arrow heads) was enhanced. d) Persistent enhancement was seen in the delayed phase. e) It was depicted as a complete contrast defect by CT during arterial portography (CTAP).

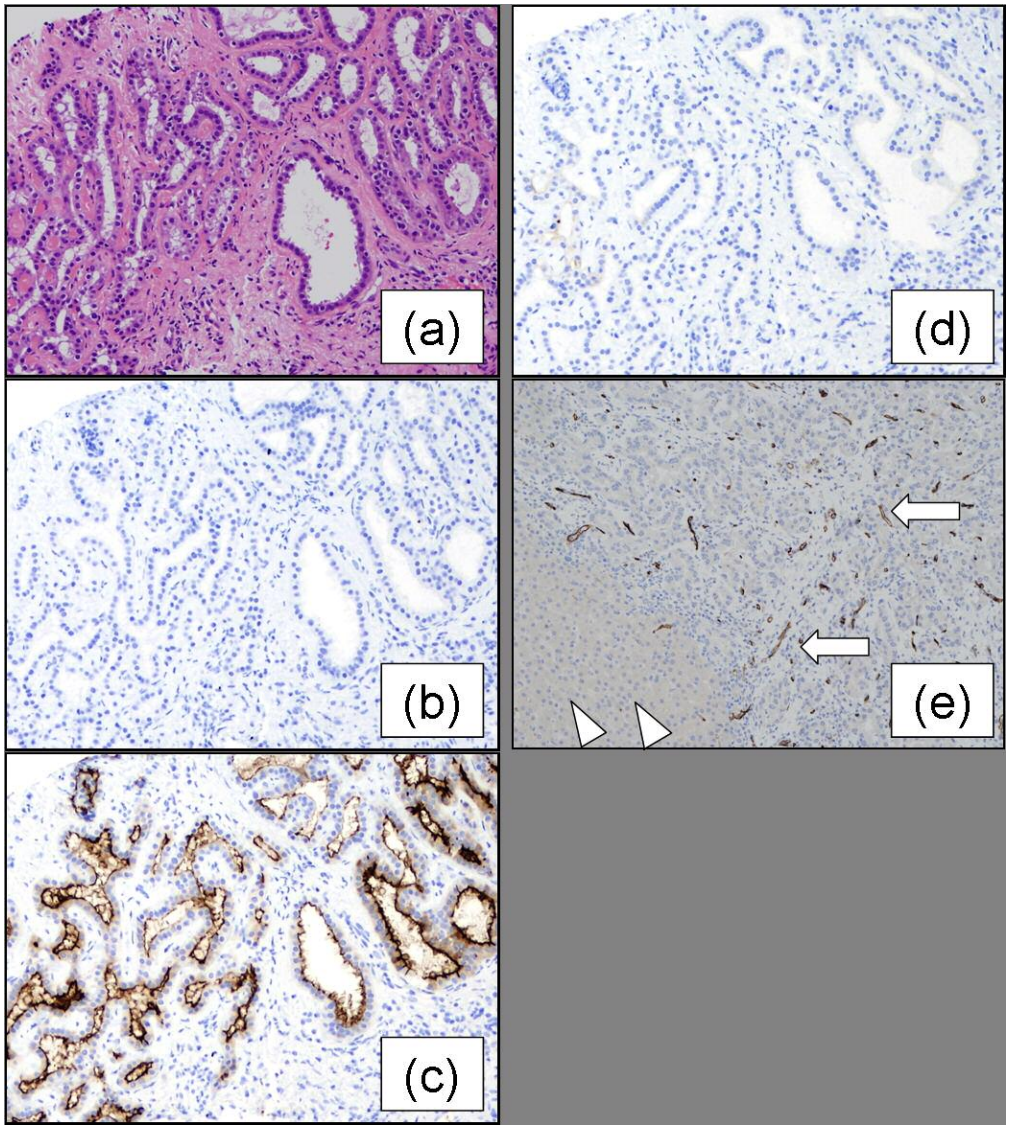

Fig. 4. a) Microscopic examination revealed that the tumor was a well differentiated adenocarcinoma. The tumor was composed of small ovoid nuclei and eosinophilic cytoplasm with mild atypia and proliferated in an anastomosing pattern of Hering's canal-like small glands with fibrous stroma. We could not see production of mucinous fluid in ducts. H & E, x100 b) Cells were immunohistologically negative to antibodies against hepatocyte paraffin 1 (Hep Par 1). x100 c) They also showed a strong intraluminal staining pattern of the gland for epithelial membrane antigens (EMA). x100 d) Cells were slightly positive for cytokeratin 19. e) A number of capillary endothelial vessels stained with antibody for CD 34 antigens were seen in the cancerous part (arrows) compared with the non-cancerous part (arrowheads). x25